# Comparison of two compressor technologies for air-source heat pumps under climate conditions of Chile

*Cynthia Rozas[a], Daniel Sacasas[b] and Cristian Cuevas[c]*

[a] *Departamento Ingeniería Mecánica, Universidad de Concepción, Concepción, Chile, cyrozas@udec.cl*
[b] *Departamento Ingeniería Mecánica, Universidad de Concepción, Concepción, Chile, dsacasas@udec.cl*
[c] *Departamento Ingeniería Mecánica, Universidad de Concepción, Concepción, Chile, crcuevas@udec.cl*

**Abstract:**

This article presents a parametric analysis for an air source heat pump using fixed speed and vapour-injected compressors. The refrigerant used is R410A and the system is evaluated under two different climate conditions from cities located in central and southern Chile: Santiago and Concepción. The compressor is modelled under a semi-empirical approach, and the parameters of the model are identified using catalogue data. The model can predict the refrigerant mass flow rate and the compressor input power with an error lower than 2% and 4% respectively. The condenser is discretised into three zones, and the heat transfer coefficients and pressure drops are determined with correlations obtained from literature. The condenser model is validated with catalogue data, and it can predict the heating power with an error lower than 3%. In the case of the evaporator, it is modelled using two zones on the refrigerant side and dry and wet regimes on the air side. The convective heat transfer coefficients and frictional pressure drops are determined using correlations obtained from literature. Finally, the evaporator fan is modelled using a polynomial approach based on the dimensionless pressure, power and flow factors. The constants of the model are identified using catalogue data. The heating load is determined for a paired-one floor house of 42,8×2 = 85,6 $m^2$. The insulation level is defined according to the Chilean thermal normative. Simulation results for a fixed speed compressor allowed to obtain a Seasonal Performance Factor (SPF) of 2,86 for Santiago and 2,92 for Concepción. Vapour-injected compressor allows to increase the SPF up to 3,13 for Santiago and 3,19 for Concepción, an improvement of 9% and an energy consumption reduction of the order on 8%.

**Keywords:**

Heat pump; Heating Space; Domestic Hot Water.

# 1. Introduction

Heat pumps have emerged as a promising technology for residential heating and Domestic Hot Water, considered a key technology in the energy transition systems while offering significant energy savings and reduced greenhouse gas emissions (Hosseini et al. [1]; Olympios et al. [2]; Vivian et al. [3]), and even more compared to conventional systems such as pellet and wood stoves. Among the common configurations, air-source heat pumps (ASHPs) are attractive due to their relatively low installation cost and widespread applicability. However, their performance is strongly influenced by climatic conditions, system design, and compressor technology, which makes detailed modelling and parametric analysis essential for assessing their suitability in diverse residential contexts. Olympios et al. [2] appointed the need of modelling approaches such as the optimization of critical components and entire heat pumps, and simulations of the effects of heat pump integration into broader multi-energy-vector systems at household.

Most of middle size heat pumps use scroll compressors due to their higher volumetric efficiency and lower noises. Fixed-speed compressors often face limitations in air-source heat pumps due to the high compressor discharge temperature. The impact of this temperature can be reduced using a vapour-injected compressor, which can also enhance the system performance, allowing a wider operating envelope (El Samad et al. [4]), particularly under colder climates where conventional ASHPs struggle to maintain efficiency, or under extreme operating conditions (Tello-Oquendo et al. [5]). Vapour injection allows for improved refrigerant mass flow and reduced discharge temperatures, leading to higher heating capacity and better seasonal performance factors (SPF). A recent work of Y. Hu and B. Shen [6] studied cold-climate heat pump using tandem compressors with and without vapour injection, confirming the need to evaluate capacity retention, efficiency, defrost behaviour, and component behaviour under realistic operating conditions. Therefore, the sizing, selection and parameter

setup of vapour-injected compressors in real conditions is still a significant issue due to the lack of information regarding how compressors will perform in all kinds of climates, where the Chilean climate context plays a key role in the national energy transition.

Accurate modelling of heat pump components is critical for predicting system behaviour under real operating conditions. Semi-empirical models based on physical principles and validated with catalogue data, provide a reliable base to estimate keys performance figures such as the Seasonal Performance Factor and the energy consumptions of energy systems based on heat pumps.

The present work provides a comprehensive assessment of the potential of two compressor technologies under two different climate conditions representative of central and southern Chile: Santiago and Concepción. By combining semi-empirical modelling with catalogue data validation, the study seeks to quantify the energetic improvements achievable with vapour injection.

# 2. Methodology

## 2.1. Household characteristics

The household considered in this study is social paired household with floor area of 42,8 $m^2$ each one. Figure 1 presents the plan view of the household, which is assumed to be perfectly aligned with the cardinal coordinates.

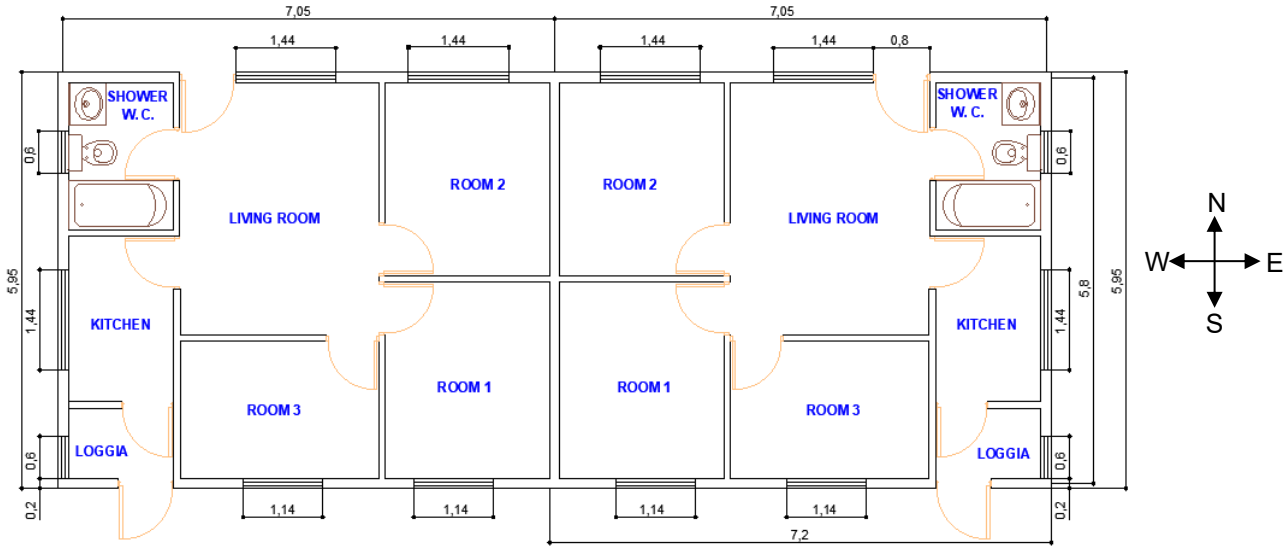


***Figure. 1.*** *Dimensions of the household (in m).*

The heating demand of the household is determined with TRNSYS considering a heating period from April to October with a constant internal temperature of 21ºC for the heated space.

The household is divided into two zones to determine the heating demand, one for the INTERIOR zone and other one for the ATTIC.

***Table 1.*** *Characteristics and dimensions of the walls and windows of the INTERIOR zone.*

| | Orientation | Total area (Incl. windows) $m^2$ | % of Window | Layers |
|---|---|---|---|---|
| External walls | North | 35,25 | 19% | Stucco, Brick, Stucco, Insulation |
| | East | 29 | 0 | |
| | South | 35,25 | 15% | |
| | West | 29 | 15% | |
| Internal Walls | - | 150 | 0 | Plasterboard, Wood, Plasterboard |
| Ceiling | - | 40,89 | 0 | Plasterboard, expanded polystyrene |
| Floor | - | 40,89 | 0 | Reinforced concrete |

## 2.2. Climate conditions

Two different climate conditions are considered for the cities of Santiago and Concepción, the first one located in central Chile and the second one in southern Chile. Santiago is classified as Csb (Warm-summer Mediterranean climate) and Concepción Cfb, but in some cases it is considered as Cfb (Temperate oceanic climate). Table 2 summarizes the monthly average, minimum and maximum temperature, as well as the monthly solar radiation.

***Table 2.*** *Climate conditions for Santiago and Concepción.*

| | Santiago | | | | Concepción | | | |
|---|---|---|---|---|---|---|---|---|
| Month | $t_{av}$ ºC | $t_{min}$ ºC | $t_{max}$ ºC | $I_{month}$ kWh/m² | $t_{av}$ ºC | $t_{min}$ ºC | $t_{max}$ ºC | $I_{month}$ kWh/m² |
| Jan | 21,5 | 10,7 | 33,9 | 241 | 16,6 | 8,0 | 26,3 | 217 |
| Feb | 20,5 | 9,5 | 31,6 | 192 | 16,3 | 8,1 | 25,2 | 165 |
| Mars | 18,8 | 6,8 | 31,5 | 163 | 15,0 | 5,3 | 24,1 | 140 |
| Apr | 14,6 | 3,9 | 29,3 | 107 | 12,2 | 3,1 | 22,3 | 89 |
| May | 10,8 | 0,4 | 25,2 | 73 | 10,5 | 1,5 | 20,2 | 55 |
| Jun | 8,6 | -0,6 | 21,5 | 54 | 9,5 | 1,1 | 16,9 | 43 |
| Jul | 8,4 | -1,6 | 21,8 | 68 | 9,0 | 1,0 | 17,0 | 52 |
| Aug | 9,8 | -0,1 | 23,5 | 87 | 9,6 | 1,7 | 18,4 | 76 |
| Sept | 11,6 | 0,5 | 23,9 | 123 | 10,1 | 1,8 | 19,9 | 109 |
| Oct | 15,0 | 3,9 | 27,9 | 172 | 12,0 | 4,1 | 20,0 | 155 |
| Nov | 17,4 | 6,0 | 29,3 | 217 | 13,5 | 5,0 | 22,5 | 185 |
| Dec | 20,0 | 8,7 | 32,0 | 241 | 15,6 | 6,2 | 24,2 | 207 |

## 2.3. Energy demands

### 2.3.1. Heating demand

The heating demand determined with the TRNSYS model is presented in Table 3, classified by monthly and annual demand for the two cities considered. The heating demand considers both paired households.

***Table 3.*** *Heating demand for Santiago and Concepción.*

| | Santiago | Concepción |
|---|---|---|
| Month | $Q_{demand}$ kWh | $Q_{demand}$ kWh |
| Jan | 0 | 0 |
| Feb | 0 | 0 |
| Mars | 0 | 0 |
| Apr | 298 | 700 |
| May | 1131 | 1262 |
| Jun | 1639 | 1467 |
| Jul | 1658 | 1575 |
| Aug | 1312 | 1337 |
| Sept | 824 | 1067 |
| Oct | 277 | 711 |
| Nov | 0 | 0 |
| Dec | 0 | 0 |
| Annual | 7139 | 8119 |

The heating demand per floor area are 83,3 kWh/m² for the household located in Santiago and 94,8 kWh/m² for the household located in Concepción.

### 2.3.2. Domestic Hot Water demand

The Domestic Hot Water energy demand is determined using the profile proposed by the ASHRAE [7], presented in Figure 2, assuming that the hot water must be supplied at 55ºC.

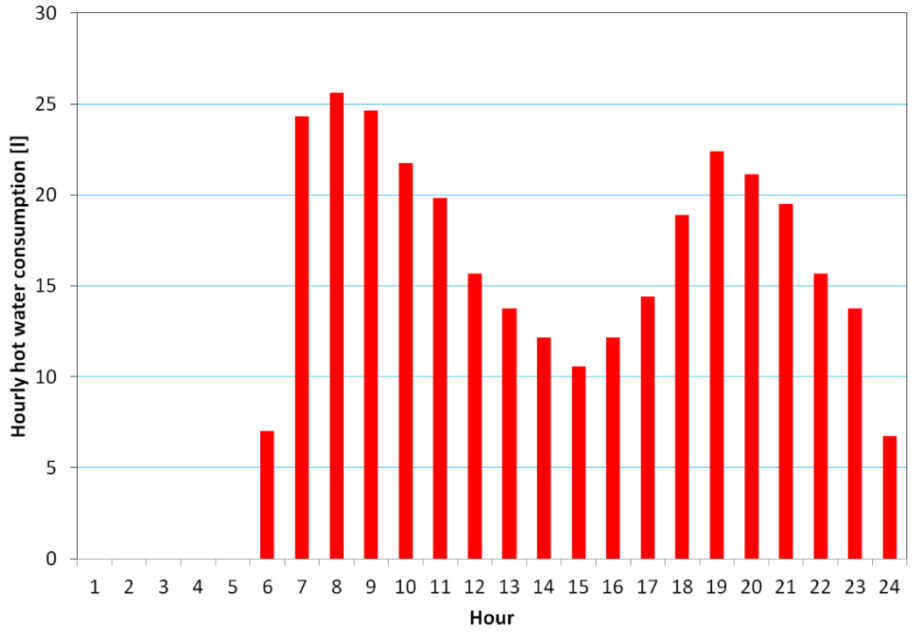


***Figure 2.*** *Domestic Hot Water profile.*

The energy demand obtained for the Domestic Hot Water is summarized in Table 4 summarized classified by month and the total annual demand. It considers the energy demand of both paired households.

***Table 4.*** *Domestic Hot Water energy demand for Santiago and Concepción.*

| | Santiago | Concepción |
|---|---|---|
| Month | $DHW_{demand}$ kWh | $DHW_{demand}$ kWh |
| Jan | 687 | 747 |
| Feb | 790 | 853 |
| Mars | 540 | 575 |
| Apr | 544 | 570 |
| May | 584 | 602 |
| Jun | 580 | 591 |
| Jul | 604 | 613 |
| Aug | 597 | 609 |
| Sept | 561 | 580 |
| Oct | 558 | 586 |
| Nov | 519 | 554 |
| Dec | 520 | 563 |
| Annual | 7082 | 7442 |

## 2.4. Heat pump modelling

The heat pump is modelled using a modular approach, using semi-empirical approaches to model the compressor, the condenser, the evaporator and the axial fan. The working fluid used in this modelling is R410A, refrigerant that is used in this domain but that is phasing-out due to its higher GWP.

### 2.4.1. Compressor model

#### 2.4.1.1. Fixed speed compressor

A 220 V scroll compressor is considered for the heat pump. The modelling approach used in this study is the one proposed by Winandy et al. [8]. It is assumed that the compressor imposes the refrigerant mass flow rate, its input power and the refrigerant exhaust temperature.

The mass flow rate of refrigerant entering the compressor is determined using the equation (1).

$$\dot{M}_{r,in,cp} = \frac{V_{s,cp} \cdot N_{cp}}{v_{r,su1,cp}} \quad (1)$$

It depends on the compressor swept volume, which is a model parameter that must be identified.

The compressor input power is determined as the addition of the internal compression power and the compressor electromechanical losses, according to equation (2). The internal compression power is in turn determined as the addition of the isentropic compression power and the isochoric compression poser, as indicated in equation (3). Finally, the compressor electromechanical losses are determined with a semi-empirical relationship depending on the internal compression power, defined in equation (4).

$$\dot{W}_{cp} = \dot{W}_{in,cp} + \dot{W}_{loss,cp} \quad (2)$$

$$\dot{W}_{in,cp} = \dot{M}_{r,in,cp} \cdot \left[\left(h_{r,ad,cp} - h_{r,su2,cp}\right) + v_{r,ad,cp} \cdot \left(P_{r,ex3,cp} - P_{r,ad,cp}\right)\right] \quad (3)$$

$$\dot{W}_{loss,cp} = \dot{W}_{loss0,cp} + \alpha \cdot \dot{W}_{in,cp} \quad (4)$$

The intermediate specific volume between the isentropic and isochoric compression $v_{r,ad,cp}$ is determined with equation (5).

$$r_{v,in,cp} = \frac{v_{r,su1,cp}}{v_{r,ad,cp}} \quad (5)$$

In these equations $\dot{W}_{loss0,cp}$, $\alpha$ and $r_{v,in,cp}$ are parameters of the model that must be identified.

### 2.4.1.2. Vapour injected compressor

The base of the vapour-injected compressor model is the same presented previously. The difference is in the way that injected refrigerant mass flow rate is considered in the modelling. In this case, the approach proposed by Winandy and Lebrun [9] is considered, who assume that the injection is carried out just after the closure of the suction pocket. Thus, a new state $su2$ is defined by the mixing of the refrigerant mass flow rate coming from the evaporator and injected mass flow rate, as indicated in equation (6).

$$h_{su2} = \frac{\dot{M}_{r,cp} \cdot h_{r,su1,cp} + \dot{M}_{r,inj,cp} \cdot h_{r,inj,cp}}{\dot{M}_{r,cp}} \quad (6)$$

Where the refrigerant mass flow rate exhausting the compressor is given by:

$$\dot{M}_{r,tot,cp} = \dot{M}_{r,cp} + \dot{M}_{r,inj,cp} \quad (7)$$

The injection pressure and the injected refrigerant mass flow rate are determined with the empirical relationships presented in equations (8) and (9).

$$P_{r,inj} = a_0 + a_1 \cdot P_{r,cd} + a_2 \cdot P_{r,ev} \quad (8)$$

$$\frac{\dot{M}_{r,inj}}{\dot{M}_{r,cp}} = b_0 + b_1 \cdot P_{r,inj} + b_2 \cdot P_{r,cd} \quad (9)$$

Where $a_i$ and $b_i$ are constants of the empirical relationships that must be identified from catalogue data.

## 2.4.2. Condenser model

The condenser is modelled using a three-zones approach, as proposed by Cuevas et al. [10], and considering a plate heat exchanger. The three zones are defined by the refrigerant state in superheated zone, two-phase zone and subcooled zone. Each zone is evaluated through their energy balances on the refrigerant and on the water sides. The $\varepsilon - NTU$ method is used to determine the fluid-to-fluid heat transfer. Equations (10), (11) and (12) present the $\varepsilon - NTU$ method applied to the superheated zone, which at the same time is applied for the two-phase and subcooled zones.

$$\dot{Q}_{r,sh,cd} = \dot{M}_{r,cd} \cdot \left(h_{r,su,sh,cd} - h_{r,ex,sh,cd}\right) \quad (10)$$

$$\dot{Q}_{w,sh,cd} = \dot{M}_{w,cd} \cdot \left(h_{w,ex,sh,cd} - h_{w,su,sh,cd}\right) \quad (11)$$

$$\dot{Q}_{sh,cd} = \varepsilon_{sh,cd} \cdot \dot{C}_{min,sh,cd} \cdot \left(t_{r,su,sh,cd} - t_{w,su,sh,cd}\right) \quad (12)$$

The heat exchanger effectiveness in this zone is determined by considering a counterflow configuration, as indicated in equation (13).

$$\varepsilon_{sh,cd} = \frac{1-exp\left[-NTU_{sh,cd}\cdot\left(1-\omega_{sh,cd}\right)\right]}{1-\omega_{sh,cd}\cdot exp\left[-NTU_{sh,cd}\cdot\left(1-\omega_{sh,cd}\right)\right]} \quad (13)$$

The two-phase and the subcooled zones are evaluated with the same equations, but in the case of the two-phase zone the effectiveness is determined as indicated in equation (14).

$$\varepsilon_{tp,cd} = 1 - exp\left[-NTU_{tp,cd}\right] \quad (14)$$

This model imposes the condensing pressure and allows to determine the heat flows and heat transfer areas of each zone, as indicated in equations (15), (16) and (17).

$$\dot{Q}_{cd} = \dot{Q}_{sh,cd} + \dot{Q}_{tp,cd} + \dot{Q}_{sc,cd} \quad (15)$$

$$A_{r,cd} = A_{r,sh,cd} + A_{r,tp,cd} + A_{r,sc,cd} \quad (16)$$

$$A_{w,cd} = A_{w,sh,cd} + A_{w,tp,cd} + A_{w,sc,cd} \quad (17)$$

## 2.4.3. Evaporator model

The evaporator is modelled in a similar way than the condenser, but in this case a two zones model is considered: two-phase and superheating zones. The main difference is on the air side, because in this side there are several possibilities with the humidity present in the moist air. If the surface temperature is higher than the air dew point temperature, there will be no condensation on the air side. If only a partial part of the evaporator surface has a temperature lower than the dew point temperature, there will be a part of the surface under dry conditions and the other part under wet conditions. If the entire surface has a temperature lower that the dew point, the entire surface will be under wet conditions. Finally, if part or the total surface temperature of the evaporator is lower than 0ºC, in that part there will be frost formation. In this modelling only dry and wet conditions will be considered. These conditions are modelled as proposed by Braun [11] and Ding et al. [12], who propose to determine the heat transfer in the evaporator assuming that it is working under a completely dry regime or under a completely wet regime, using the higher of these two values.

$$Q_{ev} = MAX\left(Q_{dry,coil};\ Q_{wet,coil}\right) \quad (18)$$

According to Braun, this assumption introduces an error lower than 5%. For the dry regime the analysis is similar to the one presented for the condenser. The difference is in case of the wet regime due to the water condensation of the moist air, which introduce a combined heat-mass transfer mechanism.

For wet conditions a fictitious ideal gas is defined to model the mist air, which allows to define the energy balance on the air side as defined in equations (19) and (20).

$$\dot{Q}_{a,wet,coil} = \dot{M}_{a,coil}\cdot\left(h_{a,su,wet,coil} - h_{a,ex,wet,coil}\right) - \dot{M}_{a,coil}\cdot\left(W_{a,su,wet,coil} - W_{a,ex,wet,coil}\right)\cdot h_{wl,coil} \quad (19)$$

$$\dot{Q}_{a,wet,coil} = \dot{C}_{fa,wet,coil}\cdot\left(t_{wb,su,wet,coil} - t_{wb,ex,wet,coil}\right) \quad (20)$$

The heat transfer fluid-to-fluid is determined using the $\varepsilon - NTU$ method, using the same assumptions presented for the condenser.

The air conditions at the evaporator exhaust are determined as proposed by ASHRAE [13], who considers that the conditions of the exhaust air are the result of the mixture of the air entering to the evaporator and the air in contact with the evaporator surface, which assumed to be saturated at a temperature equal to the evaporator surface temperature. This assumption is summarized in equations 21 to 24.

$$h_{a,su,wet,coil} - h_{a,ex,wet,coil} = \varepsilon_{c,wet,coil}\cdot\left(h_{a,su,wet,coil} - h_{c,wet,coil}\right) \quad (21)$$

$$W_{a,su,wet,coil} - W_{a,ex,wet,coil} = \varepsilon_{c,wet,coil}\cdot\left(W_{a,su,wet,coil} - W_{c,wet,coil}\right) \quad (22)$$

$$\varepsilon_{c,wet,coil} = 1 - exp\left(-NTU_{c,wet,coil}\right) \quad (23)$$

$$NTU_{c,wet,coil} = \frac{1}{R_{a,coil} \cdot \dot{C}_{a,dry,coil}} \quad (24)$$

## 2.4.4. Fan model

The fan is modelled using a model based in three dimensionless factors: pressure factor, flow factor and power factor, which are defined in equations 25, 26 and 27 respectively.

$$\psi = \frac{\Delta P_{total}}{\rho \frac{U^2}{2}} \quad (25)$$

$$\phi = \frac{\dot{V}}{A \cdot U} \quad (26)$$

$$\lambda = \frac{\phi \cdot \psi}{\varepsilon_s} \quad (27)$$

The model is then based on two polynomials laws depending on one of these three factors, which is taken as independent variable. In this case the flow factor is taken as independent variable and the polynomial laws are the ones presented in equations (28) and (29).

$$\lambda_{fan} = a_0 + a_1 \cdot \phi_{fan} + a_2 \cdot \phi_{fan}^2 \quad (28)$$

$$\phi_{fan} = b_0 + b_1 \cdot \phi_{fan} + b_2 \cdot \phi_{fan}^2 \quad (29)$$

## 2.4.5. Heat pump model

The heat pump model is obtained integrating all sub-models of each component, which are interconnected with their corresponding inputs and outputs, as presented in Figure 3. In order to achieve the heating capacity, it is assumed that the heat pump works with an ON/OFF control, where the compressor and fan speeds have two options: the nominal speed or zero.

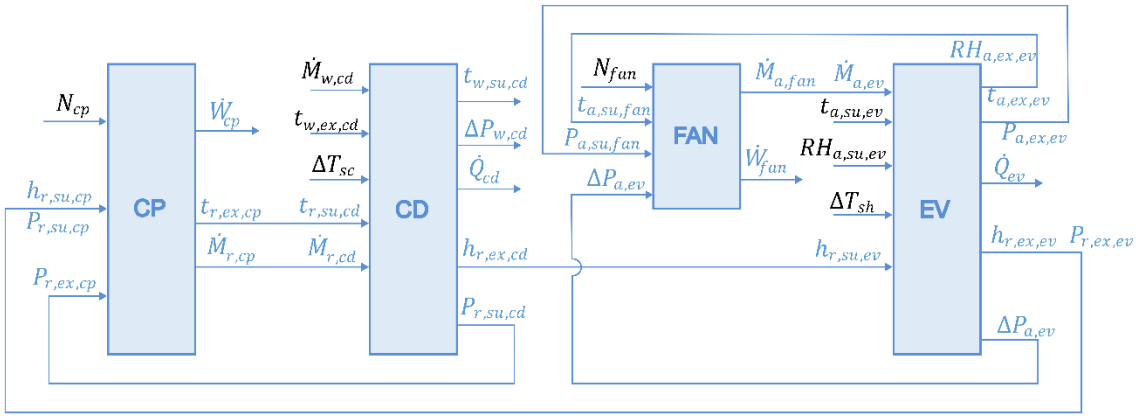


***Figure 3.*** *Modelling principle of the heat pump.*

# 2.5. Model validation

The parameters of the fixed speed and vapour-injected compressor models are determined from the commercial compressor manufactured by Copeland, models ZH5 and ZHI5 respectively. Figure 4 presents the prediction of the compressor input power for both compressors. The Root Mean Square Error in the prediction of the refrigerant mass flow rate was 1% for the ZH5 compressor and 4% for the ZHI5 compressor, in the prediction of the compressor input power 3% for the ZH5 compressor and 4% for the ZHI5 compressor, and finally for the prediction of the compressor exhaust temperature 1,7 K % for the ZH5 compressor and 2,5K for the ZHI5 compressor.

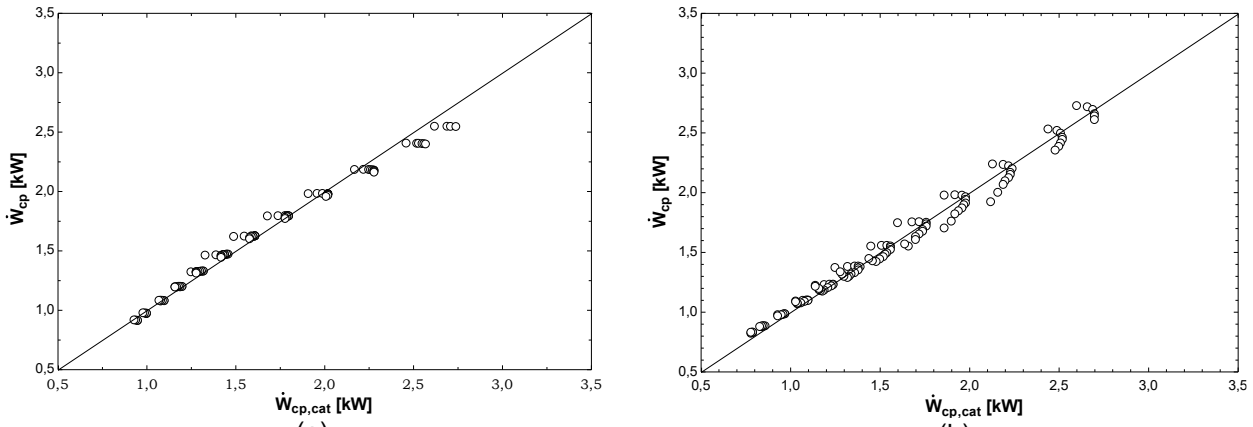


***Figure 4.*** *Prediction of the compressor input power for the (a) fixed speed compressor and (b) vapour-injected compressor.*

The dimensions considered for the condenser and the evaporator are presented in Table 5, which are used to determine the heat transfer areas and convective coefficients for the refrigerant side, the air side, and the water side. For the condenser, the dimensions of the Alfa Laval condenser model CBH60-16H-F are taken as a reference.

***Table 5.*** *Dimensions of the evaporator and condenser.*

| Evaporator | | Condenser | |
|---|---|---|---|
| Variable | Dimension | Variable | Dimension |
| Tube external diameter | 9,53 mm | Number of plates | 45 |
| Tube thickness | 0,81 mm | Active width of 1 plate | 0,083 |
| Longitudinal pitch | 21 mm | Active height of 1 plate | 0,433 m |
| Transversal pitch | 25 mm | Plate thickness | 0,32 mm |
| Number of rows | 4 | Plate pitch | 2 mm |
| Number of circuits | 2×2 | Chevron angle | 60º |
| Number of tubes per row | 11 | Enlargement factor | 1,25 |
| Fin thickness | 0,3 mm | | |
| Fin pitch | 2 mm | | |
| Heat exchanger height | 0,55 m | | |
| Heat exchanger depth | 0,084 m | | |
| Heat exchanger width | 0,786 m | | |
| Total number of tubes | 88×2 | | |

The constants of the axial fan model were identified from the catalogue data for the fan model W3G-400 from the manufacturer ebm-papst.

The heat pump model is not validated with catalogue data or with experimental results, it is only presented the performance obtained under different climate conditions for a given water exhaust temperature of 55ºC. Figure 5 presents the results obtained for heating and COP. An influence of the ambient relative humidity is observed in both results due to the water condensation on the evaporator surface. The model does not consider the effect of frost formation on the evaporator surface.

# 3. Results and discussion

Figure 6 and Figure 7 present the system COP throughout the year for the two systems analysed operating under the weather conditions of Santiago and Concepción.

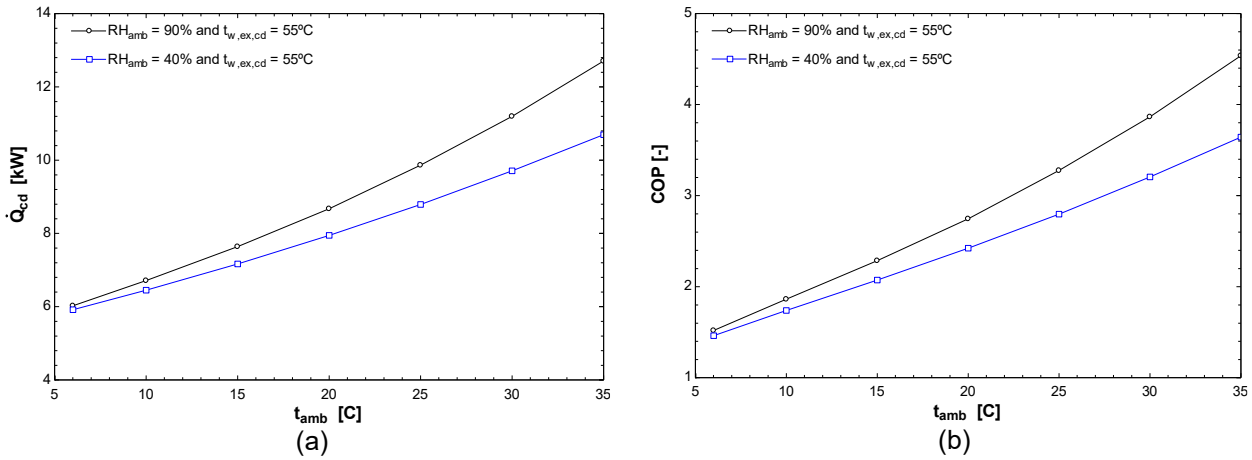


***Figure 5.*** *Hourly heat pump COP for Santiago with (a) a fixed speed compressor and (b) a vapour-injected compressor.*

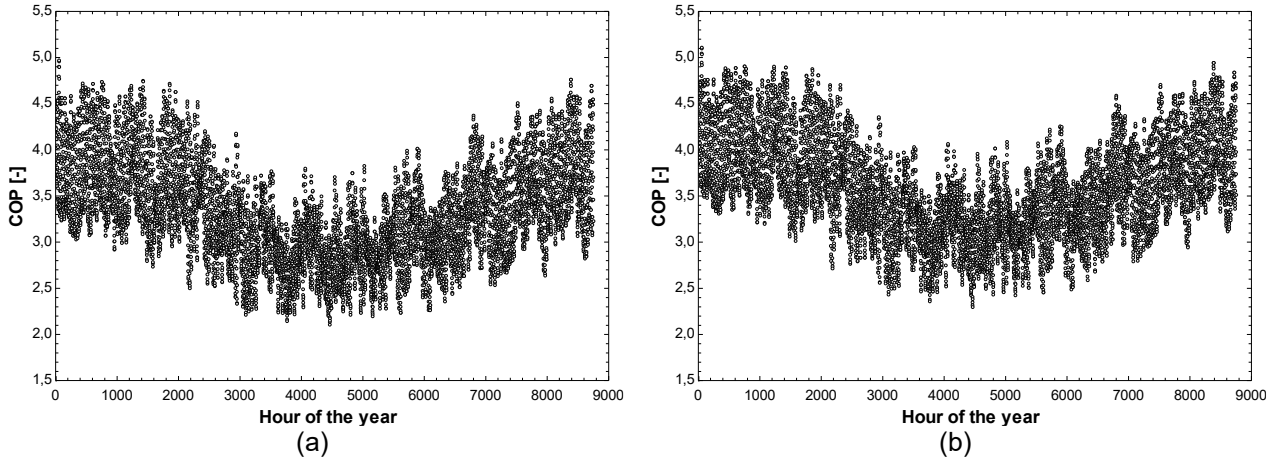


***Figure 6.*** *Hourly heat pump COP for Santiago with (a) a fixed speed compressor and (b) a vapour-injected compressor.*

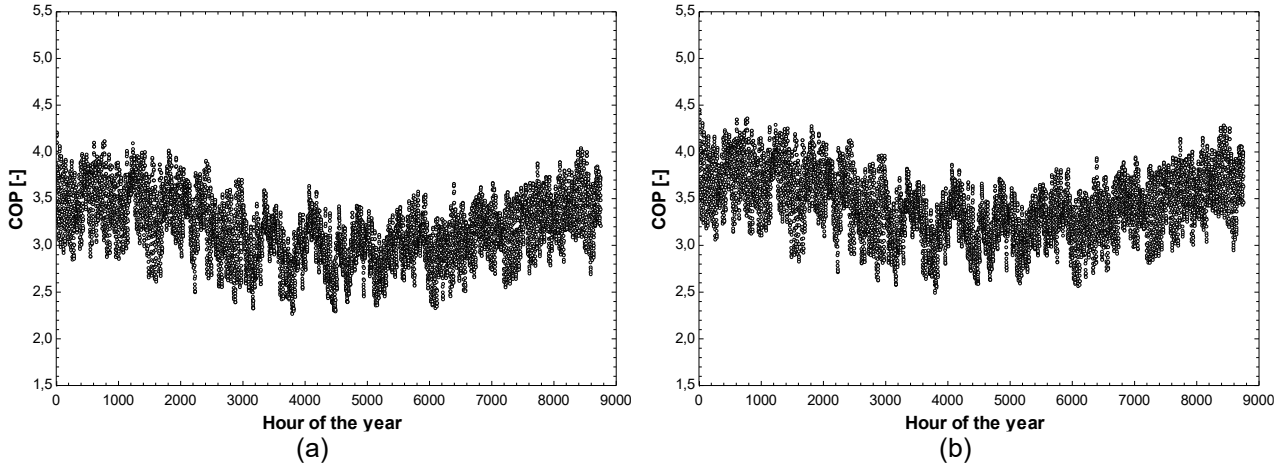


***Figure 7.*** *Hourly heat pump COP for Concepción with (a) a fixed speed compressor and (b) a vapour-injected compressor.*

In both cases, with the fixed speed and vapour injection compressor, it is assumed that the heat pump works under an ON/OFF regulation. The Seasonal Performance Factor of the heat pump is determined using equation (30).

$$SPF = \frac{\sum_{i=1}^{8760} \dot{Q}_{demand,i} \cdot \Delta\tau_i}{\sum_{i=1}^{8760} (\dot{W}_{cp,fl,i} + \dot{W}_{fan,i}) \cdot \Delta\tau_i} \quad (30)$$

Where $\Delta\tau_i$ is the fraction of time of the hour $i$ that the heat pump is in ON mode, $\dot{Q}_{demand,i}$ is the total demand (heating + DHW) in the hour $i$, and $\dot{W}_{cp,fl,i}$ and $\dot{W}_{fan,i}$ are the compressor power at full load and the fan power at the hour $i$.

The results obtained from the simulations are summarized in Table 6.

***Table 6.*** *Results of the annual simulation.*

| City | Compressor type | Heating + DHW demand [kWh] | Heat supplied by the heat pump [kWh] | Heat pump Consumption [kWh] | SPF |
|---|---|---|---|---|---|
| Santiago | Fixed speed compressor | 10680 | 10677 | 3731 | 2,86 |
| | Vapour-injected compressor | 10680 | 10680 | 3410 | 3,13 |
| Concepción | Fixed speed compressor | 11839 | 11839 | 4048 | 2,92 |
| | Vapour-injected compressor | 11839 | 11839 | 3717 | 3,19 |

According to the results, using a vapour injected compressor allows to reduce the energy consumption in 8% and to increase the Seasonal Performance Factor in 9%.

# 4. Conclusions

A semi empirical model was developed to evaluate the performance of a heat pump working with a fixed speed compressor and a vapour-injected compressor in an air source heat pump used for heating and Domestic Hot Water for a social dwelling located in two different Chilean cities: Santiago and Concepción. The evaluated system allows to cover almost 100% of the heating and Domestic Hot Water demand, with the system using a vapour injected compressor presenting a Seasonal Performance Factor 9% lower than the system using a fixed speed compressor and a 8% lower energy consumption,

# Acknowledgments

This study was funded by the Chilean research agency ANID through the research project FONDECYT regular 1251412.

# Nomenclature

| | |
|---|---|
| $A$ | area, $m^2$ |
| $a_i$ | constants |
| $b_i$ | constants |
| $\dot{C}$ | capacity flow, $W \cdot K^{-1}$ |
| $COP$ | Coefficient Of Performance |
| $DHW$ | Domestic Hot Water |
| $h$ | specific enthalpy, $J \cdot kg^{-1}$ |
| $I$ | solar radiation, $W\ m^{-2}$ |
| $\dot{M}$ | mass flow rate, $kg\ s^{-1}$ |
| $N$ | rotational speed, $s^{-1}$ |
| $P$ | pressure, Pa |
| $Q$ | heat, J |
| $\dot{Q}$ | heat flow, W |
| $R$ | thermal resistance, $K \cdot W^{-1}$ |
| $r$ | ratio |

| | |
|---|---|
| $SPF$ | Seasonal Performance Factor |
| $t$ | temperature, ºC |
| $V$ | volume, $m^3$, or value |
| $v$ | specific volume, $m^3\ kg^{-1}$ |
| $W$ | humidity ratio, $kg{\cdot}kg^{-1}$ |
| $\dot{W}$ | power, W |

**Subscripts**

| | |
|---|---|
| $a$ | air |
| $ad$ | adapted condition |
| $av$ | average |
| $c$ | contact |
| $cat$ | catalogue |
| $cp$ | compressor |
| $cd$ | condenser |
| $coil$ | heat exchanger |
| Demand | demand |
| $dry$ | dry regime |
| $ev$ | evaporator |
| $ex$ | exhaust |
| $in$ | internal |
| $loss$ | loss |
| $min$ | minimum |
| $r$ | refrigerant |
| $s$ | isentropic or swept |
| $sc$ | subcooled |
| $sh$ | superheated |
| $su$ | supply |
| $tp$ | two-phase |
| $v$ | isochoric |
| $w$ | water or wall |
| $wb$ | wet bulb |
| $wet$ | wet regime |

**Greek symbols**

| | |
|---|---|
| $\alpha$ | power loss coefficient |
| $\Delta$ | difference |
| $\varepsilon$ | effectiveness |
| $\lambda$ | power factor |
| $\phi$ | flow factor |
| $\psi$ | pressure factor |

# References


[1] Hosseini S. A., Ahmadi R., Rahmani A. Integrated gas heat pump (GHP) system for residential complexes: modeling cooling, hot water, and electricity generation. Energy Conversion and Management: X 2026, 29: 1014

[2] Olympios. A. V., Sapin P., Mersch M., Magharabi A. M., Markides C. N. A review of recent progress in the design and integration of domestic heat pumps. Next Energy 2024, 5: 100163

[3] Vivian J., Prataviera E., Cunsolo F., Pau M. Demand Side Management of a pool of air source heat pumps for space heating and domestic hot water production in a residential district. Energy Conversion and Management 2020, 225: 113457.

[4] El Samad T., Żabnieńska-Góra A., Jouhara H., Sayma A. I. A review of compressors for high temperature heat pumps. Thermal Science and Engineering Progress 2024, 51:102603

[5] Tello-Oquendo F. M., Navarro-Peris E., Gonzálvez-Maciá, J. Comparison of the performance of a vapor-injection scroll compressor and a two-stage scroll compressor working with high pressure ratios. Applied Thermal Engineering 2019, 160: 114023.

[6] Hu Y., Shen B. High-performance cold-climate heat pump using tandem compressors with and without vapor injection: Laboratory investigation and field demonstration. Energy and Buildings 2026, 358: 117218.

[7] ANSI/ASHRAE Standard 90.2, Energy-Efficient Design of Low-Rise Residential Buildings, American Society of Heating, Refrigerating and Air-Conditioning Engineers, Inc.

[8] Winandy E., Saavedra C., Lebrun J. Experimental analysis and simplified modelling of a hermetic scroll refrigeration compressor. Applied Thermal Engineering 2002, 22: 107–120.

[9] Winandy, E. L., Lebrun, J. Scroll compressors using gas and liquid injection: experimental analysis and modelling. International Journal of Refrigeration 2002, 25: 1143–1156.

[10] Cuevas C., Lebrun J., Lemort V., Ngendakumana P. Development and validation of a condenser three zones model. Applied Thermal Engineering 2009, 29: 3542–3551.

[11] Braun J.E., Klein S.A., Mitchell J.W. Effectiveness models for cooling towers and cooling coils. ASHRAE Transactions 1989. 95: 164–174.

[12] Ding X., Eppe J., Lebrun J., Wasacz M. Cooling Coil Models to be used in Transient and/or Wet Regimes. Theoretical Analysis and Experimental Evaluation, in: Proceedings of the Third International Conference on System Simulation in Buildings, Liege, pp. 405–441, 1990.

[13] ASHRAE, Air-cooling and dehumidifying coils, in: ASHRAE Handbook-HVAC Systems and Equipment, American Society of Heating, Refrigerating, and Air-Conditioning Engineers, Atlanta, pp. 23.1-23.16, 2012.